ANALYTICAL POTENTIAL SOLUTIONS FOR ESIs USING SPHEROIDAL HEAD MODELS

Zeynep Akalın, Nevzat G. Gençer
Middle East Technical University, 06531, Ankara, Turkey
zakalin@eee.metu.edu.tr, ngencer@metu.edu.tr

Abstract- *Electrical activity in the human brain can be monitored using electrodes placed on the scalp. Activity representations using voltage measurements is called electrical source image (ESI). ESIs are obtained by comparing the measurements with the solutions obtained using a numerical model of the head. Spheroid approximates the shape of a human head and can be used for that purpose. In this study, the analytical formulation for the solution of the potential distribution due to a current dipole in a uniformly conductive spheroidal head model is implemented. The accuracy in solutions is tested with the results obtained using Boundary Element Method (BEM) with a dense mesh. The solutions of analytical and numerical potential fields are compared as the depth of the dipole inside the spheroid is increased. The comparison is done for two types of spheroids: prolate spheroid (egg-shape) and oblate spheroid (discus-shape). It is observed that for prolate spheroid the error is about 1% when the dipole is not located close to boundary and for the oblate spheroid the error is calculated as approximately 3%. It is concluded that spheroid head models can be used in electro-magnetic source imaging.*

Keywords: Boundary Element Method, potential field, oblate, prolate, spheroid.

1. INTRODUCTION

Representations of the active cell populations on the cortical surface via electrical measurements is known as electrical source images (ESIs) of the human brain. Finding electrical sources from electrical measurements is the *inverse problem*. The *forward problem* of ESI is the solution of the potential distribution on the head surface for a known source distribution. The inverse problem is based on the comparison of the measurements with the calculated fields. Therefore, to be able to obtain reliable solutions of the inverse problem, the forward problem must be solved accurately [1,2]. For realistic head models, however, analytical solutions do not exist. Therefore complicated numerical methods such as the Boundary Element Method (BEM) and the Finite Element method (FEM) have to be employed to solve the potential distribution [2,3].

In general, spherical head models are used to obtain a source estimate without requiring high computing resources. However, analytical solutions are also available for head models with special geometries (concentric spheres, eccentric spheres, spheroid, etc.) [4-12]. Concentric and eccentric spheres models include more than one type of tissue, thus better than a uniform sphere. However, the solution time is higher compared to the solution using a spherical head model. A spheroidal model, on the other hand, has uniform conductivity and has the computational advantages of the spherical model while representing the head geometry better than a sphere. The analytical potential formulation of spheroid is given in [13,14]. The aim of this study is to implement this analytical formulation and test the accuracy in solutions. This will allow us to use the spheroidal head models for future inverse problem studies. The accuracy of the analytical solutions is tested with the numerical solutions of BEM that gives accurate results for a dense mesh [15].

In this study, first the analytical formulations are given for the potential field for prolate and oblate spheroidal geometries. The results include the comparison of the analytical and numerical solutions.

2. ANALYTICAL CALCULATION OF THE POTENTIAL FIELD

The potential distribution due to a current dipole can be formulated for two types of spheroids, namely, prolate and oblate spheroids [13,14]. In this section, these formulations will be summarized.

2.1 Prolate Spheroid

Figure 1 shows the coordinate system for a prolate spheroid. The prolate spheroidal coordinates (ξ, η, φ) can be related to the rectangular coordinates (x, y, z) by

$$\begin{aligned} x &= C\sqrt{(1-\xi^2)(\eta^2-1)}\sin\varphi \\ y &= C\sqrt{(1-\xi^2)(\eta^2-1)}\cos\varphi \\ z &= C\xi\eta \end{aligned} \tag{1}$$

where the prolate spheroidal coordinates are in the ranges $-1\le\xi\le1$, $1\le\eta$, $0\le\varphi<2\pi$ and C is a constant.

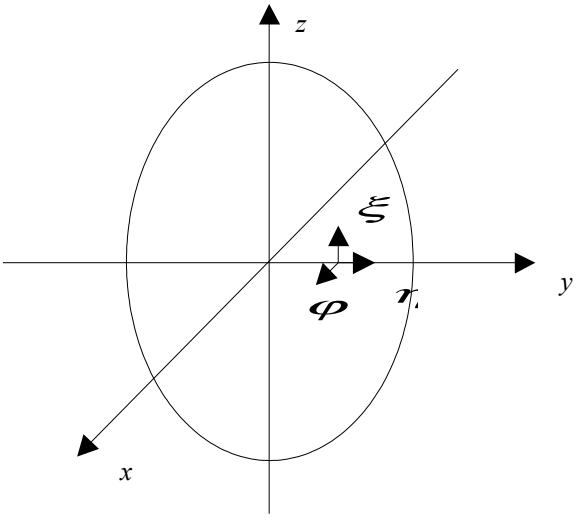

Figure 1 : Rectangular and prolate spheroidal coordinates in the case of a prolate spheroid volume conductor.

The potential field can then be calculated using the following formula [13,14]:

$$V = \frac{1}{4\pi\sigma C^2}\sum_{l=0}^{\infty}\sum_{k=0}^{l}\frac{(2-\delta_k^0)(2l+1)(l-k)!P_l^k(\xi)}{(\eta_a^2-1)(l+k)!P_l^{k\,\otimes}(\eta_a)}\times\left[\frac{P_{\xi_0}P_l^k(\eta_0)P_l^{k\,\otimes}(\xi_0)\cos k(\varphi-\varphi_0)}{h_{\xi_0}}\right.$$
$$\left.+\frac{P_{\eta_0}P_l^{k\,\otimes}(\eta_0)P_l^k(\xi_0)\cos k(\varphi-\varphi_0)}{h_{\eta_0}}+\frac{P_{\varphi_0}P_l^k(\eta_0)P_l^k(\xi_0)k\sin k(\varphi-\varphi_0)}{h_{\varphi_0}}\right] \tag{2}$$

Where P_{ξ_0}, P_{η_0}, P_{φ_0} are the current dipole moments along ξ, η, φ directions. ξ_0, η_0, φ_0 refer to the direction of the dipole and ξ, η and φ refer to the field points. The metric coefficients are

$$h_\xi = C\sqrt{\frac{\eta^2 - \xi^2}{1-\xi^2}}$$
$$h_\eta = C\sqrt{\frac{\eta^2 - \xi^2}{\eta^2 - 1}} \tag{3}$$
$$h_\varphi = C\sqrt{(1-\xi^2)(\eta^2 - 1)}$$

and

$$P_l^{k\circledast}(\xi_0) = \frac{\partial P_l^k(\xi_0)}{\partial \xi_0} \tag{4}$$

where P_l^k is the legendre polynomial of order l [16].

$$\sqrt{(1-\xi_0^2)}P_l^{k\circledast}(\xi_0) = \frac{-l(l+1)}{2}, \quad k = 1$$
$$= 0, \qquad k \neq 1 \tag{5}$$

If ξ_0=1 or η_0=1, then the following relations must be used in order to perform the calculations.

$$\sqrt{(\eta_0^2 - 1)}P_l^{k\circledast}(\eta_0) = \frac{-l(l+1)}{2}, \quad k = 1$$
$$= 0, \qquad k \neq 1 \tag{6}$$

2.2 Oblate Sheroid

Figure 2 shows the coordinate system for an oblate spheroid. The oblate spheroidal coordinates (ξ,, ζ, φ) can be related to the rectangular coordinates (x, y, z) by

$$x = C\sqrt{(1-\xi^2)(\zeta^2 + 1)}\cos\varphi$$
$$y = C\sqrt{(1-\xi^2)(\zeta^2 + 1)}\sin\varphi \tag{7}$$
$$z = C\xi\zeta$$

where the oblate spheroidal coordinates are in the ranges $-1 \le \xi \le 1$, $0 \le \zeta$, $0 \le \varphi < 2\pi$ and C is a constant.

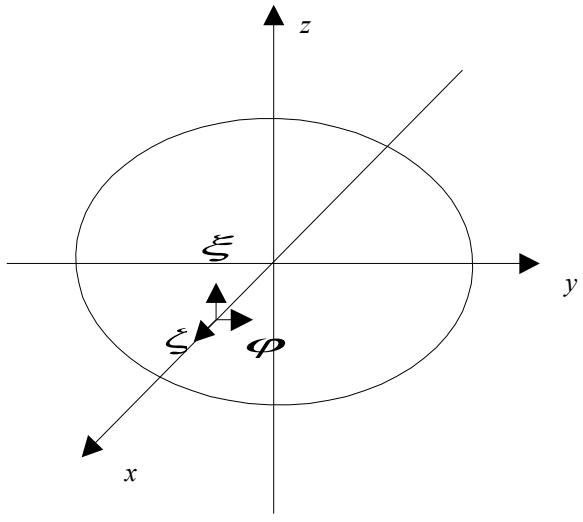

Figure 2 : Rectangular and oblate spheroidal coordinates in the case of an oblate spheroid volume conductor.

The potential field can be calculated as follows

$$V = \frac{1}{4\pi\sigma C^2}\sum_{l=0}^{\infty}\sum_{k=0}^{l}\frac{(2-\delta_k^0)(2l+1)(l-k)!P_l^k(\xi)}{(\zeta_a^2+1)(l+k)!P_l^{k\otimes}(j\zeta_a)}\times\left[\frac{P_{\xi_0}P_l^k(j\zeta_0)P_l^{k\otimes}(\xi_0)\cos k(\varphi-\varphi_0)}{h_{\xi_0}}\right.$$
$$\left.+\frac{P_{\zeta_0}P_l^{k\otimes}(j\zeta_0)P_l^k(\xi_0)\cos k(\varphi-\varphi_0)}{h_{\zeta_0}}+\frac{P_{\varphi_0}P_l^k(j\zeta_0)P_l^k(\xi_0)k\sin k(\varphi-\varphi_0)}{h_{\varphi_0}}\right] \quad (8)$$

Where P_{ξ_0}, P_{ζ_0}, P_{φ_0} are the current dipole moments along ξ, ζ, φ directions. ξ_0, ζ_0, φ_0 refer to the direction of the dipole and ξ, ζ and φ refer to the field points. The metric coefficients are

$$h_\xi = C\sqrt{\frac{\zeta^2+\xi^2}{1-\xi^2}}$$
$$h_\eta = C\sqrt{\frac{\zeta^2+\xi^2}{\zeta^2+1}} \quad (9)$$
$$h_\varphi = C\sqrt{(1-\xi^2)(\zeta^2+1)}$$

The values of the associated Legendre polynomials are calculated using MATLAB's functions and for complex values the polynomials are calculated using the recurrence relationships which are in agreement with the values available in standart tables [16].

3. NUMERICAL CALCULATION OF THE POTENTIAL FIELD USING BEM

In BEM, the entire volume (i.e., torso or human head) is subdivided into compartments with constant material properties. In bioelectric studies, material property is the electrical conductivity of tissues and it is assumed isotropic in BEM formulations. BEM transforms the differential equation that represents the electric potential due to an impressed current source in a conductive body into an integral equation over the boundary surfaces which separate regions with different conductivities. The surface integrals are calculated numerically by dividing the surface into elements. In the literature different kinds of elements and methods are used to evaluate the surface integrals [2]. This study uses the isoparametric elements proposed by Tanzer and Gençer [1,2,3]. Using isoparametric elements in the formulations enables us to express both the global coordinates and potentials on an element using the same interpolation (shape) functions. Each integration on a surface element is written as a linear combination of unknown node potentials. If the potential ϕ is to be calculated at M nodes, then in matrix notation, it is possible to obtain the following matrix equation:

$$\Phi = \mathbf{g} + \mathbf{C}\Phi \quad (10)$$

where Φ is an $M \times 1$ vector of node potentials, $\mathbf{C}$ is an $M \times M$ matrix whose elements are determined by the geometry and electrical conductivity information, and $\mathbf{g}$ is an $M \times 1$ vector representing the contribution of the primary sources. The details of the BEM formulation can be found in [1,2,3].

Figure 3 shows prolate and oblate spheroidal meshes with 512 quadratic elements.

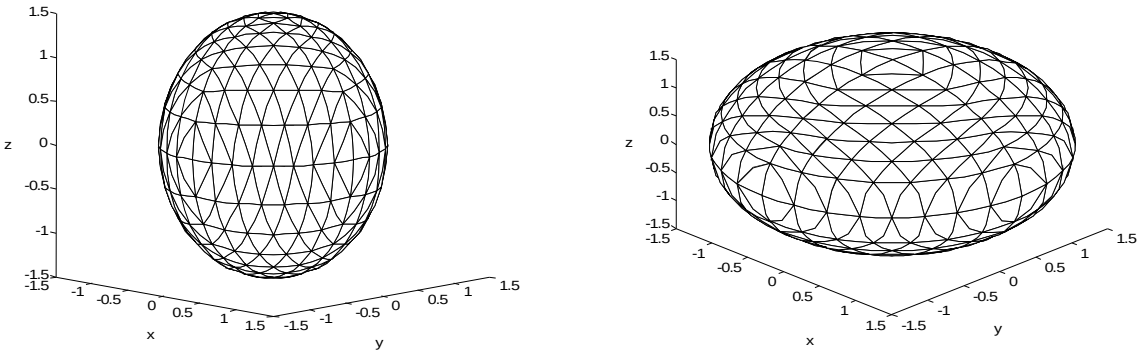

(a) (b)

Figure 3 : The prolate and oblate spheroidal meshes with 512 elements and 1026 nodes (a) prolate spheroid, (b) oblate spheroid.

4. RESULTS

The comparison of analytical potential with numerical potential obtained with BEM on the spheroid are done for prolate (at $\eta=\eta_a$) and oblate (at $\zeta=\zeta_a$) spheroids for a dipole located on z axis in ξ direction. The location of the dipole is changed from 0 to 1.4 with 0.1 steps and at each step relative difference measure (RDM) is calculated [17]. In Figure 4 the RDM plots are given for prolate and oblate spheroids with respect to the location of the dipole in z direction.

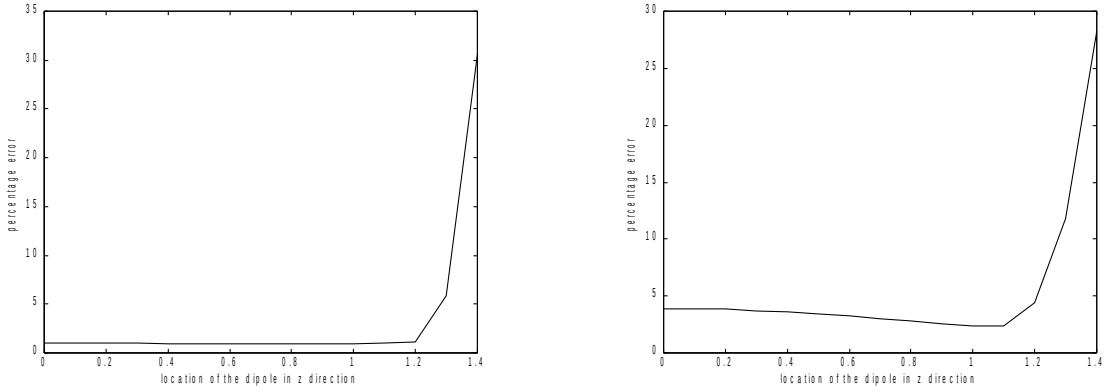

(a) (b)

Figure 4 Relative difference measures between the analytical and numerical potential solutions. The dipole is located in ξ direction on z axis at z=0,0.1,0.2,…1.4 (a) for prolate spheroid with η_a=1.5 (b) for oblate spheroid with ζ_a=1.5.

In the analytical solution of potential for prolate and oblate spheroid the summations on l are taken from 1 upto 18 for prolate spheroid and 21 for oblate spheroid. For l=0, the potential is zero [], after 17 for prolate spheroid and 21 for oblate spheroid the change in the potential is almost zero. Therefore, it is enough to take the summations upto 17 or 21. In Figure 5 the potentials are plotted with respect to l for oblate and prolate spheroid at node 20. It is seen that after l=14 for prolate spheroid and l=20 for oblate spheroid the change in the potential decreases to 0.5% of the change in the potential for l=1.

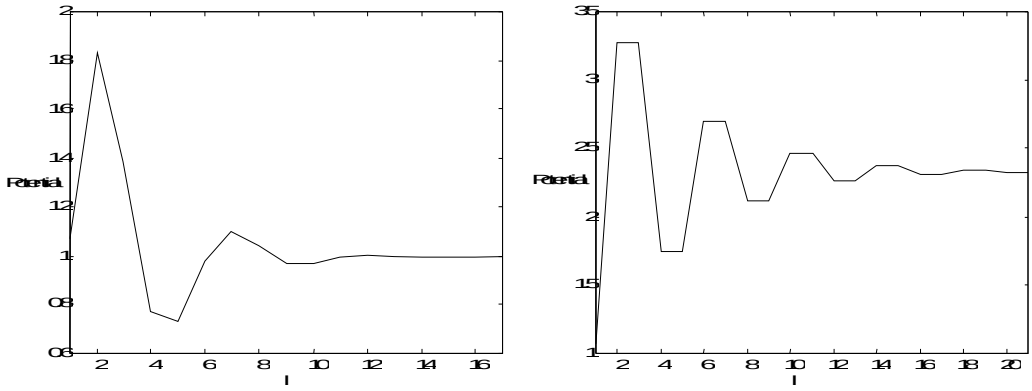

(a) (b)

Figure 5. Analytical potential calculated at one node to show how the potential changes as *l* increases (a) for prolate spheroid, (b) for oblate spheroid.

The accuracy of the analytical potentials are tested with the numerical solutions of BEM using a mesh having 512 quadratic, isoparametric elements and 1026 nodes. The numerical solutions of BEM are tested with the analytical solutions of a sphere and are known to give accurate results with approximately 1% error [1,15]. The reason for using quadratic elements is that it is possible to obtain accurate results using 512 elements. With linear elements, to obtain accurate results, a denser mesh should be used [15].

4. CONCLUSION

In this study, the analytical formulations for the solution of the potential distributions due to a current dipole in uniformly conductive spheroids are implemented. The accuracy in solutions is tested with the results obtained using Boundary Element Method (BEM) with a mesh having 512 quadratic elements. The solutions of analytical and numerical potential fields are compared as the depth of the dipole inside the spheroid is increased. The comparison is done for prolate and oblate spheroids.

For prolate spheroid the error is calculated as 1 % for dipole locations between $z = 0$ and $z = 1.1$. For dipole locations greater than $z = 1.1$ the error increases dramatically. For oblate spheroid, the error decreases from 3.5 % (at $z = 0$) to 2.5 % (at $z = 1.1$). For dipole locations greater than $z = 1.1$ the error increases as in the prolate spheroid case. It is observed that in oblate spheroid the error is larger than in prolate spheroid case for the dipole locations between 0 and 1.1 in z direction. This may be caused by the BEM meshes used for prolate and oblate spheroids. It may be possible to increase the accuracy in BEM solutions for the oblate case using a different mesh structure, however, this is still under investigation.

The BEM solutions for spherical head models reveal that the error increases for sources located nearby the head surface [1]. It is also stated in [19] that, the maximum error in BEM occurs when the dipoles approach to the head surface closer than the mean triangle edge length. In this study, similar behavior is observed for spheroids. It is concluded that the numerical results are not accurate for shallow dipoles in spheroids. Consequently, the analytical solutions for spheroidal head models can be used instead of BEM models for the future inverse problem solutions.

ACKNOWLEDGEMENT

We would like to thank Prof. Dr. Pekcan Ungan of Biophysics Department of Hacettepe, Ankara, Turkey, for attracting our attention to this problem.

REFERENCES

1. Gençer N. G., Tanzer I. O., "Forward problem solution of electromagnetic source imaging using a new BEM formulation with high-order elements," Phys. Med. Biol., 44, 1999, 2275-2287
2. Gencer N.G., Acar C.E., Tanzer I. O., Ozdemir M. K., "Forward Problem Solution of Magnetic Source Imaging", Chapter Study for Magnetic Source Imaging (Sam Williamson festschrift), Submitted, 2000
3. Gencer, N. G., "Forward Problem Solution of the Electromagnetic Source Images of the Human Brain", Submitted to Brain Machine200 Workshop.
4. Geselowitz D. B., "Model studies of the electric and magnetic fields of the heart," Jour. Franklin. Inst., 296(6), 1973, 379-391
5. Grynszpan F., Geselowitz D. B., "Model studies of the magnetocardiogram," Biophys. J., 13, 1973, 911-925.
6. Rush S., Driscoll D. A., "EEG electrode sensitivity_An application of reciprocity," IEEE Trans. Biomed. Eng., 16, 1969, 15-22.
7. Schneider M., "Effect of inhomogeneities on surface signals coming from a cerebral current dipole source," IEEE Trans. Biomed. Eng., 1974, 52-54.
8. Kavanagh R. N., Darcey T. M., Lehmann D., Fender D. H., "Evaluation of method for three-dimensional localization of electrical sources in the human brain," IEEE Trans. Biomed. Eng., 25, 1978, 421-429.
9. Sidman R. D., Giambalvo V., Allison T., Bergey P., "A method for localization of sources of human cerebral potentials evoked by sensory stimuli," Sensory Proc, 2, 1978, 116-129.
10. Cuffin N. B., "Effects of head shape on EEG's and MEG's," IEEE Trans. Biomed. Eng., 37(1), 1990, 44-51.
11. Cuffin N. B., "Eccentric spheres models of the head," IEEE Trans. Biomed. Eng., 38(9), 1991, 871-878.
12. Cuffin N. B., "EEG Localization accuracy improvements using realsitically shaped head models," IEEE Trans. Biomed. Eng., 43(3), 1996, 299-303.
13. Berry P.M. "N, M Space Harmonics of the Oblate Spheroid", Annals New York Acad. Of Sci., 65, 1126-1134, 1956.
14. Cuffin B. N., Cohen D., "Magnetic Fields of a Dipole in Special Volume Conductor Shapes", IEEE Trans. On Biomed. Imag., BME-24(4), 1977, 372-381
15. Tanzer I. O., Forward Problem Solution of Electro-Magnetic Source Imaging of the Human Brain Using a New Boundary Element Method Formulation With Realistic Head Model, Ms Thesis, Middle East Technical University, Ankara, 1998
16. Smythe W. R., Static and Dynamic Electricity, McGraw-Hill, New York, 1968
17. Meijs J. W., Weier O. W., Peters M. J., Van Oosterom A, "On the numerical accuracy of the boundary element method," IEEE Trans. Biomed. Eng., 36(10), 1038-1049, 1989
18. Lin J. C., Durand D. M., "Magnetic Field of Current Monopoles in Prolate and Oblate Spheroid Volume Conductors", IEEE Trans. On Magnetics, 34(4), 1998, 2177-2184
19. Fuchs M., Wischmann H-A., Wagner M., Theiβen A., "Performance of Realistically Shaped Boundary Element Method Volume Conductor Models", Proceedings of the 11th International Conference on Biomagnetism, 1999, 193-196